# Extension to lower energies of the cosmic-ray energy window at the Pierre Auger Observatory

G. Silli, D. Melo, D. Ravignani, M. Roth | November 2, 2021

ITeDA-KIT

# Motivation

- Photon search programme down to $10^{16}$ eV :
    - contribution to the multi-messenger studies in Auger:
    - discovery of PeVatrons in the galactic center (Tibet AS-gamma, HAWC)
    - observations of UHE photons up to 1.4 PeV (LHAASO)
    - astrophysical neutrinos at the southern hemisphere

      (IceCube)

# Motivation

- Photon search programme down to $10^{16}$ eV :
    - contribution to the multi-messenger studies in Auger:
    - discovery of PeVatrons in the galactic center (Tibet AS-gamma, HAWC)
    - observations of UHE photons up to 1.4 PeV (LHAASO)
    - astrophysical neutrinos at the southern hemisphere (IceCube)
- Auger will reach the centre of mass energy of the LHC

# Motivation

- Photon search programme down to $10^{16}$ eV :
  - contribution to the multi-messenger studies in Auger:
  - discovery of PeVatrons in the galactic center (Tibet AS-gamma, HAWC)
  - observations of UHE photons up to 1.4 PeV (LHAASO)
  - astrophysical neutrinos at the southern hemisphere (IceCube)
- Auger will reach the centre of mass energy of the LHC
- Extend the energy spectrum with the surface detector measurements

$\downarrow$

observation of the second knee

# Motivation

- Photon search programme down to $10^{16}$ eV :
  - contribution to the multi-messenger studies in Auger:
  - discovery of PeVatrons in the galactic center (Tibet AS-gamma, HAWC)
  - observations of UHE photons up to 1.4 PeV (LHAASO)
  - astrophysical neutrinos at the southern hemisphere (IceCube)
- Auger will reach the centre of mass energy of the LHC
- Extend the energy spectrum with the surface detector measurements

$\downarrow$

observation of the second knee

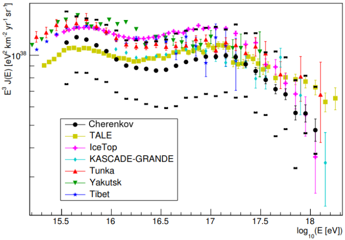

# Motivation

- Photon search programme down to $10^{16}$ eV :
  - contribution to the multi-messenger studies in Auger:
  - discovery of PeVatrons in the galactic center (Tibet AS-gamma, HAWC)
  - observations of UHE photons up to 1.4 PeV (LHAASO)
  - astrophysical neutrinos at the southern hemisphere (IceCube)
- Auger will reach the centre of mass energy of the LHC
- Extend the energy spectrum with the surface detector measurements

↓

observation of the second knee

The SD-433 will allow for the first time the measurement the three UHE spectrum features not only by a single observatory but with the same detection technique

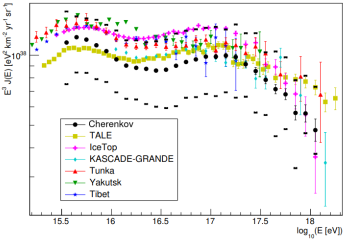


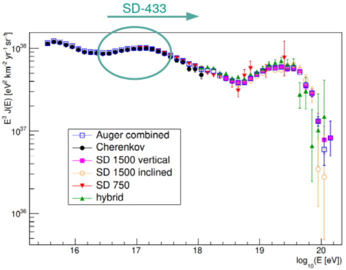

# Evolution of the SD-433

- 2013

The first hexagonal cell has been completed: six additional tanks around the central one, Tina Turner. These seven SD stations constitute the unique elementary cell of the SD433 array.
The whole hexagon became fully operational at mid May 2013.

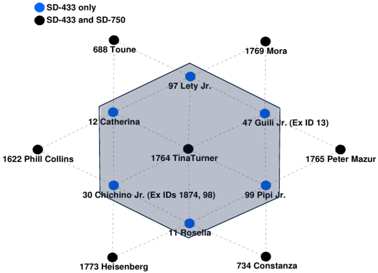

# Evolution of the SD-433

UNSAM UNIVERSIDAD NACIONAL DE SAN MARTÍN

KIT Karlsruhe Institute of Technology

- **2013** The first hexagonal cell has been completed: six additional tanks around the central one, Tina Turner. These seven SD stations constitute the unique elementary cell of the SD433 array. The whole hexagon became fully operational at mid May 2013.
- **2016** Technical Board approved the SD433 extension of the $2^{nd}$ crown on a simulation-based trigger efficiency analysis. SD-433 dedicated working group formed

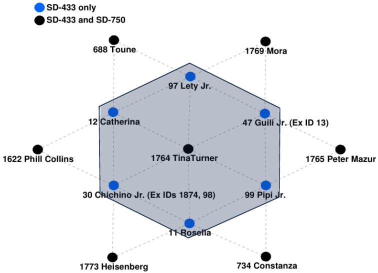

# Evolution of the SD-433

UNSAM
UNIVERSIDAD NACIONAL DE SAN MARTÍN

KIT
Karlsruhe Institute of Technology

- **2013** The first hexagonal cell has been completed: six additional tanks around the central one, Tina Turner. These seven SD stations constitute the unique elementary cell of the SD433 array.
  The whole hexagon became fully operational at mid May 2013.
- **2016** Technical Board approved the SD433 extension of the $2^{nd}$ crown on a simulation-based trigger efficiency analysis.
  SD-433 dedicated working group formed
- **2017** Upgrade of the communication systems.
  Correction of WCDs positions (98-13).

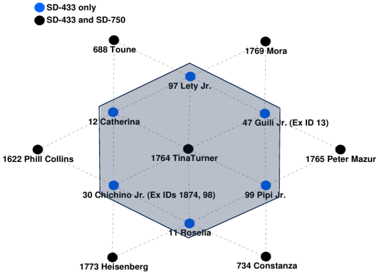

# Evolution of the SD-433

UNSAM UNIVERSIDAD NACIONAL DE SAN MARTÍN

Karlsruhe Institute of Technology

- **2013** The first hexagonal cell has been completed: six additional tanks around the central one, Tina Turner. These seven SD stations constitute the unique elementary cell of the SD433 array. The whole hexagon became fully operational at mid May 2013.
- **2016** Technical Board approved the SD433 extension of the $2^{nd}$ crown on a simulation-based trigger efficiency analysis. SD-433 dedicated working group formed
- **2017** Upgrade of the communication systems. Correction of WCDs positions (98-13).
- **2018** Three new additional WCDs(Water-Cherenkov Detectors) have been deployed (left). Fast CDAS (silent-stations) fixed.

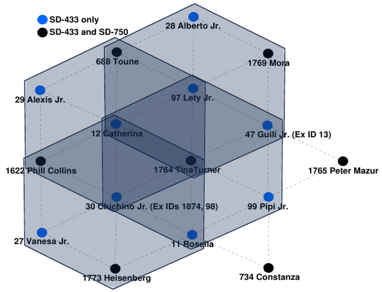

# Evolution of the SD-433

- 2013 — The first hexagonal cell has been completed: six additional tanks around the central one, Tina Turner. These seven SD stations constitute the unique elementary cell of the SD433 array.
  The whole hexagon became fully operational at mid May 2013.
- 2016 — Technical Board approved the SD433 extension of the $2^{nd}$ crown on a simulation-based trigger efficiency analysis.
  SD-433 dedicated working group formed
- 2017 — Upgrade of the communication systems.
  Correction of WCDs positions (98-13).
- 2018 — Three new additional WCDs(Water-Cherenkov Detectors) have been deployed (left). Fast CDAS (silent-stations) fixed.
- 2019 — Three more additional WCDs deployed (right).
  Seven hegagons aperture.
  The SD-433 is now completed!

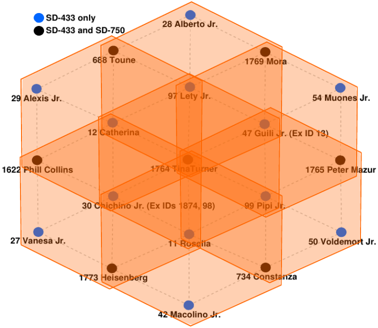

# Evolution of the SD-433

- **2013** — The first hexagonal cell has been completed: six additional tanks around the central one, Tina Turner. These seven SD stations constitute the unique elementary cell of the SD433 array.
  The whole hexagon became fully operational at mid May 2013.
- **2016** — Technical Board approved the SD433 extension of the 2$^{nd}$ crown on a simulation-based trigger efficiency analysis.
  SD-433 dedicated working group formed
- **2017** — Upgrade of the communication systems.
  Correction of WCDs positions (98-13).
- **2018** — Three new additional WCDs(Water-Cherenkov Detectors) have been deployed (left). Fast CDAS (silent-stations) fixed.
- **2019** — Three more additional WCDs deployed (right).
  Seven hegagons aperture.
  The SD-433 is now completed!

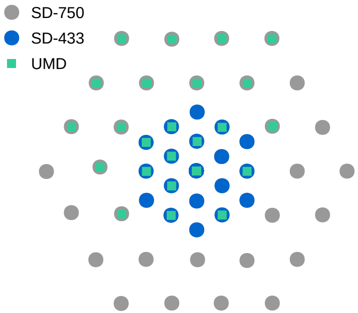

# Array efficiency

UNSAM UNIVERSIDAD NACIONAL DE SAN MARTÍN

Karlsruhe Institute of Technology

## Shower simulations

- with QGSJetII-04 as hadronic interactions model
- of 2000 proton- and 2000 iron-initiated air-showers
- continuous energy distribution as $E^{-1}$ between $4 \times 10^{16}$ eV and $10^{17}$ eV
- isotropic distribution up to $\theta = 55°$
- Offline revision 32963

# Array efficiency

UNSAM
UNIVERSIDAD NACIONAL DE SAN MARTÍN
Karlsruhe Institute of Technology

## Shower simulations

- with QGSJetII-04 as hadronic interactions model
- of 2000 proton- and 2000 iron-initiated air-showers
- continuous energy distribution as $E^{-1}$ between $4 \times 10^{16}$ eV and $10^{17}$ eV
- isotropic distribution up to $\theta = 55°$
- Offline revision 32963

The efficiency $\epsilon$:

- Array efficiency $\epsilon$ defined as the probability of reconstructing an event.
- Array efficiency fitted with:

$$\epsilon(E) = \frac{1}{2} \times \left[\mathrm{Erf}\left(a \times (\log_{10}(E_{\mathrm{MC}}/\mathrm{eV}) - 16) + b\right) + 1\right]$$

# Array efficiency

## Shower simulations

- with QGSJetII-04 as hadronic interactions model
- of 2000 proton- and 2000 iron-initiated air-showers
- continuous energy distribution as $E^{-1}$ between $4 \times 10^{16}$ eV and $10^{17}$ eV
- isotropic distribution up to $\theta = 55°$
- $\overline{\text{Off}}\underline{\text{line}}$ revision 32963

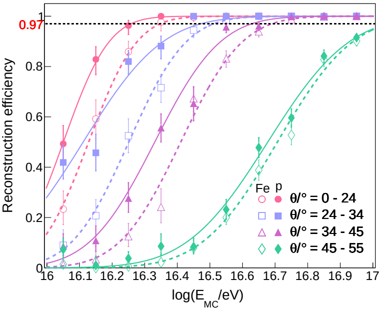


The efficiency $\epsilon$:

- Array efficiency $\epsilon$ defined as the probability of reconstructing an event.
- Array efficiency fitted with:

$$\epsilon(E) = \frac{1}{2} \times \left[\mathrm{Erf}\left(a \times (\log_{10}(E_{MC}/\mathrm{eV}) - 16) + b\right) + 1\right]$$

# Array efficiency

## Shower simulations

- with QGSJetII-04 as hadronic interactions model
- of 2000 proton- and 2000 iron-initiated air-showers
- continuous energy distribution as $E^{-1}$ between $4 \times 10^{16}$ eV and $10^{17}$ eV
- isotropic distribution up to $\theta = 55°$
- $\overline{\text{Off}}\underline{\text{line}}$ revision 32963

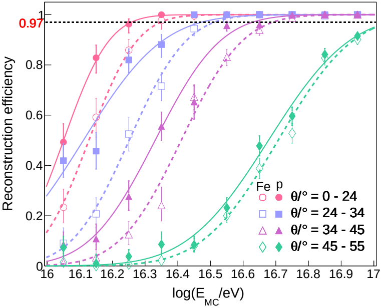


The efficiency $\epsilon$:

- Array efficiency $\epsilon$ defined as the probability of reconstructing an event.
- Array efficiency fitted with:

$$\epsilon(E) = \frac{1}{2} \times \left[\mathrm{Erf}\left(a \times (\log_{10}(E_{MC}/\mathrm{eV}) - 16) + b\right) + 1\right]$$

1. 97% efficiency above $10^{16.7}$ eV for $\theta < 45°$
   a lower energy threshold of $10^{16.5}$ eV can be reached when restricting the zenith angle up to $\theta = 35°$
2. lower energy threshold for p than for Fe
3. maximum zenith angle of 45°

# Data recovery

The Missing silent problem:

- CDAS was recording data from T3 triggered stations **only** (2013-2018)
- only T3 triggered stations in the event
- no informations on silent stations
- silent stations for
  - 6T5 condition (20K 6T5 events lost in 5 years)
  - correct determination of the shower geometry
  - perform a good LDF fit
  - proper exposure calculation
- fixed in July 20$^{th}$ 2018 (X.Bertou)

# Data recovery

The Missing silent problem:

- CDAS was recording data from T3 triggered stations **only** (2013-2018)
- only T3 triggered stations in the event
- no informations on silent stations
- silent stations for
  - 6T5 condition (20K 6T5 events lost in 5 years)
  - correct determination of the shower geometry
  - perform a good LDF fit
  - proper exposure calculation
- fixed in July 20th 2018 (X.Bertou)

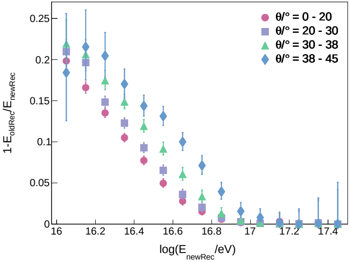

# Data recovery

The Missing silent problem:

- CDAS was recording data from T3 triggered stations **only** (2013-2018)
- only T3 triggered stations in the event
- no informations on silent stations
- silent stations for
  - 6T5 condition (20K 6T5 events lost in 5 years)
  - correct determination of the shower geometry
  - perform a good LDF fit
  - proper exposure calculation
- fixed in July 20th 2018 (X.Bertou)

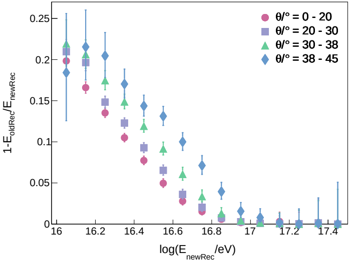


It was imperative to restore the missing silent station in all events

New module implemented in the module sequence!

- uses T2raw monitoring file informations
- looks for a match between the GPS of each event
- checks the activity status of all SD-433 WCDs
- looks for discrepancies between the "alive" stations according to the T2 files and the stations in the data
- the active non-triggered stations are added in the event as Silent

# Data recovery

The Missing silent problem:

- CDAS was recording data from T3 triggered stations **only** (2013-2018)
- only T3 triggered stations in the event
- no informations on silent stations
- silent stations for
  - 6T5 condition (20K 6T5 events lost in 5 years)
  - correct determination of the shower geometry
  - perform a good LDF fit
  - proper exposure calculation
- fixed in July 20$^{th}$ 2018 (X.Bertou)

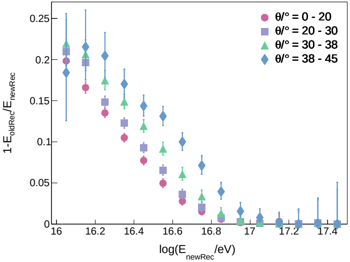


It was imperative to restore the missing silent station in all events

New module implemented in the module sequence!

- uses T2raw monitoring file informations
- looks for a match between the GPS of each event
- checks the activity status of all SD-433 WCDs
- looks for discrepancies between the “alive“ stations according to the T2 files and the stations in the data
- the active non-triggered stations are added in the event as Silent

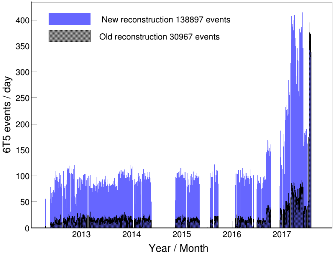

# Optimal distance

**Dataset and selection creteria**

- between May 2013 and May 2020
- asking for the 6T5 condition and no saturation

$$\downarrow$$

115 thousand events

# Optimal distance

UNSAM
UNIVERSIDAD NACIONAL DE SAN MARTÍN

Karlsruhe Institute of Technology

## Dataset and selection creteria

- between May 2013 and May 2020
- asking for the 6T5 condition and no saturation

$\downarrow$

115 thousand events

The optimal distance $r_{opt}$:

- can be estimated during the event reconstruction
- defined as the distance where model-provided signal is maximally reliable
- initial value 250 m (GAP2013_115, S.Messina)

# Optimal distance

### Dataset and selection creteria

- between May 2013 and May 2020
- asking for the 6T5 condition and no saturation

↓

115 thousand events

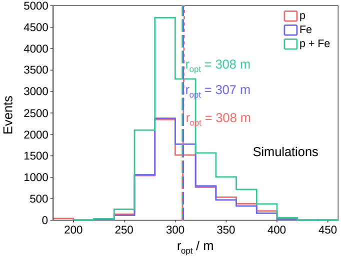


The optimal distance $r_{opt}$:

- can be estimated during the event reconstruction
- defined as the distance where model-provided signal is maximally reliable
- initial value 250 m (GAP2013_115, S.Messina)

# Optimal distance

UNSAM
UNIVERSIDAD NACIONAL DE SAN MARTÍN

KIT
Karlsruhe Institute of Technology

**Dataset and selection creteria**

- between May 2013 and May 2020
- asking for the 6T5 condition and no saturation

↓

115 thousand events

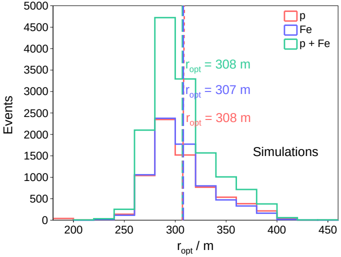


The optimal distance $r_{opt}$:

- can be estimated during the event reconstruction
- defined as the distance where model-provided signal is maximally reliable
- initial value 250 m (GAP2013_115, S.Messina)

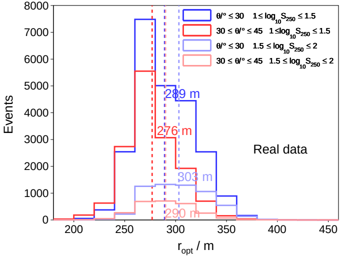

# Optimal distance

UNSAM UNIVERSIDAD NACIONAL DE SAN MARTÍN

KIT Karlsruhe Institute of Technology

## Dataset and selection creteria

- between May 2013 and May 2020
- asking for the 6T5 condition and no saturation

↓

115 thousand events

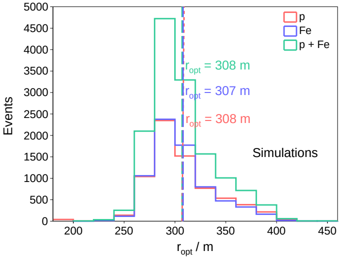


The optimal distance $r_{opt}$:

- can be estimated during the event reconstruction
- defined as the distance where model-provided signal is maximally reliable
- initial value 250 m (GAP2013_115, S.Messina)

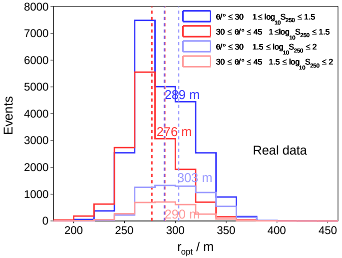


$r_{opt}$ is estimated to be about 300 m independently of the shower size and zenith angle and shower.

Compatible results obtained with real data

# Lateral distribution function

$$S(r) = S(r_{\text{opt}}) \cdot \underbrace{\left(\frac{r}{r_{\text{opt}}}\right)^{\beta} \left(\frac{r + r_{\text{opt}}}{r_{\text{scale}} + r_{\text{opt}}}\right)^{\beta}}_{f_{\text{LDF}}(r_{\text{opt}})}$$

where $f_{\text{LDF}}(r_{opt}) = 1$ and $r_{\text{scale}} = 700$ m

# Lateral distribution function

$$S(r) = S(r_{\mathrm{opt}}) \cdot \underbrace{\left(\frac{r}{r_{\mathrm{opt}}}\right)^{\beta} \left(\frac{r + r_{\mathrm{opt}}}{r_{\mathrm{scale}} + r_{\mathrm{opt}}}\right)^{\beta}}_{f_{\mathrm{LDF}}(r_{\mathrm{opt}})}$$

where $f_{\mathrm{LDF}}(r_{opt}) = 1$ and $r_{\mathrm{scale}} = 700$ m

Slope $\beta$ as free parameter if:

- Number of stations $\geq 5$
- at least two stations within $100 - 400$ m from the shower axis with $r_{max} > 225$ m or
- at least three stations within $100 - 400$ m from the shower axis with $r_{max} > 200$ m or
- at least four stations within $100 - 400$ m from the shower axis with $r_{max} > 175$ m

# Lateral distribution function

$$S(r) = S(r_{opt}) \cdot \underbrace{\left(\frac{r}{r_{opt}}\right)^{\beta} \left(\frac{r + r_{opt}}{r_{scale} + r_{opt}}\right)^{\beta}}_{f_{LDF}(r_{opt})}$$

where $f_{LDF}(r_{opt}) = 1$ and $r_{scale} = 700$ m

The event-by-event $\beta$ can be described by

$$\beta(\log S_{300}, \theta) = a(\theta) + b(\theta) \times \log_{10} S_{300}$$

$$\begin{pmatrix} a \\ b \end{pmatrix} = \underbrace{\begin{pmatrix} -1.77 \pm 0.01 & -1.61 \pm 0.01 & 1.17 \pm 0.01 \\ -0.4 \pm 0.01 & 0.78 \pm 0.01 & -0.4 \pm 0.006 \end{pmatrix}}_{\text{fit parameters}} \times \begin{pmatrix} 1 \\ \sec\theta \\ \sec^2\theta \end{pmatrix}$$

we obtain the $\hat{\beta}_i$ from the model prediction

Slope $\beta$ as free parameter if:

- Number of stations $\geq 5$
- at least two stations within $100 - 400$ m from the shower axis with $r_{max} > 225$ m or
- at least three stations within $100 - 400$ m from the shower axis with $r_{max} > 200$ m or
- at least four stations within $100 - 400$ m from the shower axis with $r_{max} > 175$ m

# Lateral distribution function

UNSAM UNIVERSIDAD NACIONAL DE SAN MARTÍN

Karlsruhe Institute of Technology

$$S(r) = S(r_{opt}) \cdot \underbrace{\left(\frac{r}{r_{opt}}\right)^{\beta}\left(\frac{r + r_{opt}}{r_{scale} + r_{opt}}\right)^{\beta}}_{f_{LDF}(r_{opt})}$$

where $f_{LDF}(r_{opt}) = 1$ and $r_{scale} = 700$ m

The event-by-event $\beta$ can be described by

$$\beta(\log S_{300}, \theta) = a(\theta) + b(\theta) \times \log_{10} S_{300}$$

$$\begin{pmatrix} a \\ b \end{pmatrix} = \underbrace{\begin{pmatrix} -1.77 \pm 0.01 & -1.61 \pm 0.01 & 1.17 \pm 0.01 \\ -0.4 \pm 0.01 & 0.78 \pm 0.01 & -0.4 \pm 0.006 \end{pmatrix}}_{\text{fit parameters}} \times \begin{pmatrix} 1 \\ \sec\theta \\ \sec^2\theta \end{pmatrix}$$

we obtain the $\hat{\beta}_i$ from the model prediction

Slope $\beta$ as free parameter if:

- Number of stations $\geq 5$
- at least two stations within 100 — 400 m from the shower axis with $r_{max} > 225$ m or
- at least three stations within 100 — 400 m from the shower axis with $r_{max} > 200$ m or
- at least four stations within 100 — 400 m from the shower axis with $r_{max} > 175$ m

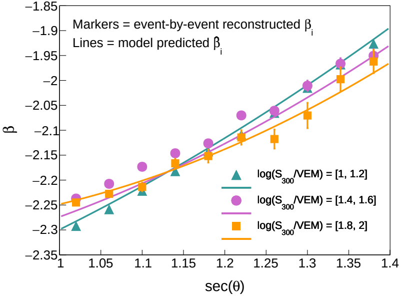

# Residuals and $\beta$ uncertainty

- Goodness of fit evaluation by comparison between reconstructed $\beta_i$ and model predictions $\hat{\beta}_i$

$$Res(\beta_i) := \frac{\beta_i - \hat{\beta}_i}{\hat{\beta}_i}$$

Model describes data with an average relative difference of 2% for the considered $S_{300}$ and $\theta$ intervals

# Residuals and $\beta$ uncertainty

- Goodness of fit evaluation by comparison between reconstructed $\beta_i$ and model predictions $\hat{\beta}_i$

$$Res(\beta_i) := \frac{\beta_i - \hat{\beta}_i}{\hat{\beta}_i}$$

Model describes data with an average relative difference of 2% for the considered $S_{300}$ and $\theta$ intervals

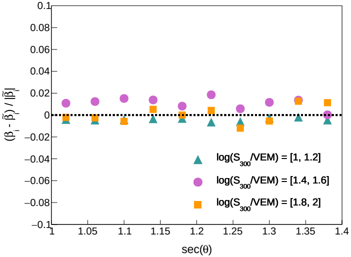

# Residuals and $\beta$ uncertainty

UNSAM UNIVERSIDAD NACIONAL DE SAN MARTÍN

KIT Karlsruhe Institute of Technology

- Goodness of fit evaluation by comparison between reconstructed $\beta_i$ and model predictions $\hat{\beta}_i$

$$Res(\beta_i) := \frac{\beta_i - \hat{\beta}_i}{\hat{\beta}_i}$$

Model describes data with an average relative difference of 2% for the considered $S_{300}$ and $\theta$ intervals

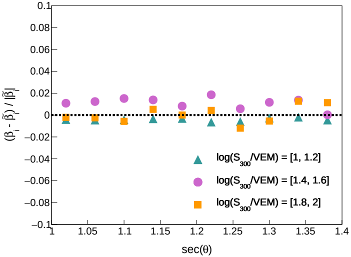


Slope fluctuations:

- the slope uncertainty model defined by

$$\sigma_\beta = \exp\left[p_0 + p_1 \cdot \log_{10}(S_{300}/\mathrm{VEM})\right]$$

with fitted parameters
$p_0 = (0.01 \pm 0.02)$ and $p_1 = (1.2 \pm 0.02)$

# Residuals and $\beta$ uncertainty

- Goodness of fit evaluation by comparison between reconstructed $\beta_i$ and model predictions $\hat{\beta}_i$

$$Res(\beta_i) := \frac{\beta_i - \hat{\beta}_i}{\hat{\beta}_i}$$

Model describes data with an average relative difference of 2% for the considered $S_{300}$ and $\theta$ intervals

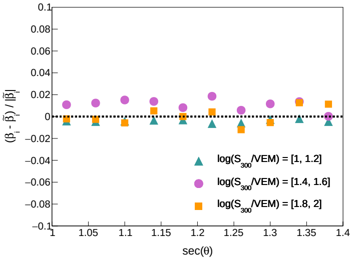


Slope fluctuations:

- the slope uncertainty model defined by

$$\sigma_\beta = \exp\left[p_0 + p_1 \cdot \log_{10}(S_{300}/\mathrm{VEM})\right]$$

with fitted parameters
$p_0 = (0.01 \pm 0.02)$ and $p_1 = (1.2 \pm 0.02)$

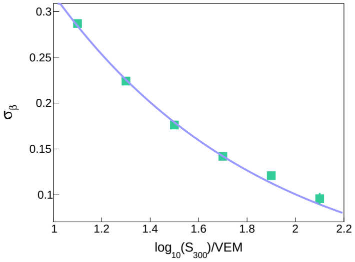

# Constant Intensity Cut

- the signal at the optimal distance $S_{r_{\text{opt}}}$ depends on the energy $E$ and on the zenith angle $\theta$ of the primary CR
- The Constant Intensity Cut (CIC) method eliminates the zenith angle dependence of $S_{r_{\text{opt}}}$
- obtain the zenith-independent energy estimator

$$S_{\theta_{\text{ref}}}(E) = \frac{S_{r_{\text{opt}}}}{\text{CIC}(\theta)}$$

$\theta_{\text{ref}} = 30°$ and $\text{CIC}(\theta) = 1 + ax(\theta) + bx^2(\theta)cx^3(\theta)$

# Constant Intensity Cut

- the signal at the optimal distance $S_{r_{\text{opt}}}$ depends on the energy $E$ and on the zenith angle $\theta$ of the primary CR
- The Constant Intensity Cut (CIC) method eliminates the zenith angle dependence of $S_{r_{\text{opt}}}$
- obtain the zenith-independent energy estimator

$$S_{\theta_{\text{ref}}}(E) = \frac{S_{r_{\text{opt}}}}{\text{CIC}(\theta)}$$

$\theta_{\text{ref}} = 30°$ and $\text{CIC}(\theta) = 1 + ax(\theta) + bx^2(\theta)cx^3(\theta)$

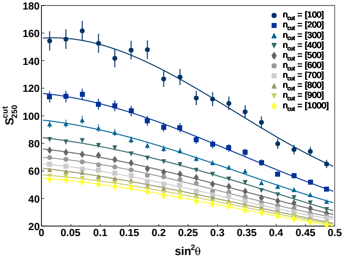

# Constant Intensity Cut

- the signal at the optimal distance $S_{r_{\mathrm{opt}}}$ depends on the energy $E$ and on the zenith angle $\theta$ of the primary CR
- The Constant Intensity Cut (CIC) method eliminates the zenith angle dependence of $S_{r_{\mathrm{opt}}}$
- obtain the zenith-independent energy estimator

$$S_{\theta_{\mathrm{ref}}}(E) = \frac{S_{r_{\mathrm{opt}}}}{\mathrm{CIC}(\theta)}$$

$$\theta_{\mathrm{ref}} = 30° \text{ and } \mathrm{CIC}(\theta) = 1 + ax(\theta) + bx^2(\theta)cx^3(\theta)$$

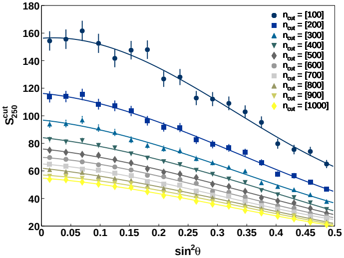


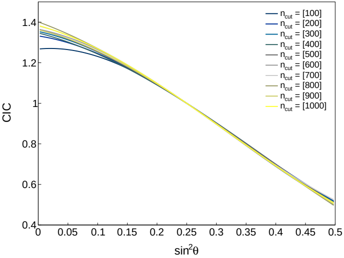

# Constant Intensity Cut

- the signal at the optimal distance $S_{r_{opt}}$ depends on the energy $E$ and on the zenith angle $\theta$ of the primary CR
- The Constant Intensity Cut (CIC) method eliminates the zenith angle dependence of $S_{r_{opt}}$
- obtain the zenith-independent energy estimator

$$S_{\theta_{ref}}(E) = \frac{S_{r_{opt}}}{\mathrm{CIC}(\theta)}$$

$$\theta_{ref} = 30° \text{ and } \mathrm{CIC}(\theta) = 1 + ax(\theta) + bx^2(\theta)cx^3(\theta)$$

The attenuation function associated with $n_{cut} = 500$ is chosen as a first estimation of the CIC corrections

| Parameter | $S_{30}^{cut}$/VEM | a | b | c |
|---|---|---|---|---|
| Value | 55.68 | -1.92 | -1.03 | 3.25 |
| Uncertainty | 0.48 | 0.09 | 0.31 | 2.23 |

| Parameter | $S_{30}^{cut}$/VEM | a | b | c |
|---|---|---|---|---|
| Value | 34.15 | -1.76 | -1.15 | 1.56 |
| Uncertainty | 0.30 | 0.09 | 0.31 | 2.27 |

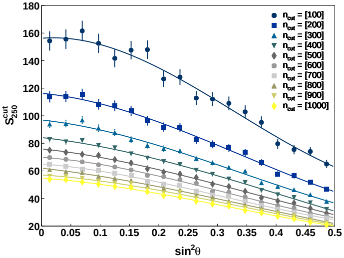


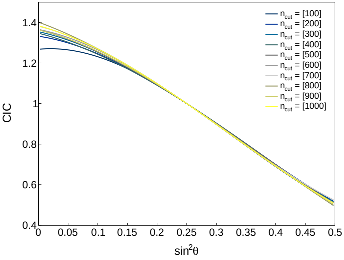

# Constant Intensity Cut

- the signal at the optimal distance $S_{r_{\mathrm{opt}}}$ depends on the energy $E$ and on the zenith angle $\theta$ of the primary CR
- The Constant Intensity Cut (CIC) method eliminates the zenith angle dependence of $S_{r_{\mathrm{opt}}}$
- obtain the zenith-independent energy estimator

$$S_{\theta_{\mathrm{ref}}}(E) = \frac{S_{r_{\mathrm{opt}}}}{\mathrm{CIC}(\theta)}$$

$$\theta_{\mathrm{ref}} = 30° \text{ and } \mathrm{CIC}(\theta) = 1 + ax(\theta) + bx^2(\theta)cx^3(\theta)$$

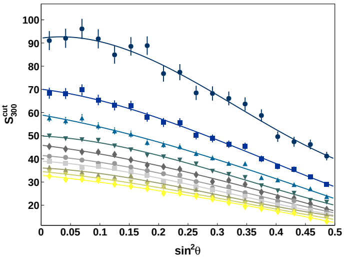


The attenuation function associated with $n_{\mathrm{cut}}$ = 500 is chosen as a first estimation of the CIC corrections

| Parameter | $S_{30}^{\mathrm{cut}}$/VEM | a | b | c |
|---|---|---|---|---|
| Value | 55.68 | -1.92 | -1.03 | 3.25 |
| Uncertainty | 0.48 | 0.09 | 0.31 | 2.23 |

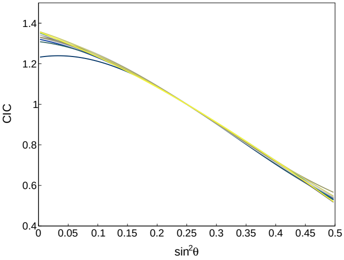


| Parameter | $S_{30}^{\mathrm{cut}}$/VEM | a | b | c |
|---|---|---|---|---|
| Value | 34.15 | -1.76 | -1.15 | 1.56 |
| Uncertainty | 0.30 | 0.09 | 0.31 | 2.27 |

# From $S_{r_{\mathbf{opt}}}$ to $S_{30}$

- With rising zenith angle the distributions are shifted to lower signals due to the increasing attenuation of the air showers
- The horizontal line corresponds to a constant intensity which is clearly not achieved for the same value of $S_{r_{\text{opt}}}$

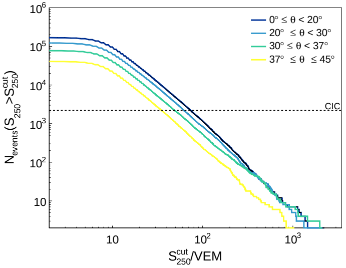

# From $S_{r_{\mathrm{opt}}}$ to $S_{30}$

- With rising zenith angle the distributions are shifted to lower signals due to the increasing attenuation of the air showers
- The horizontal line corresponds to a constant intensity which is clearly not achieved for the same value of $S_{r_{\mathrm{opt}}}$

$\downarrow$

applying the CIC correction

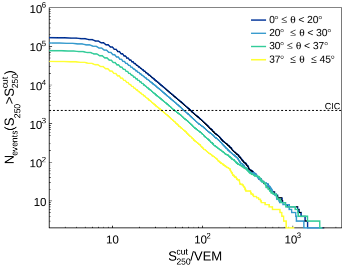

# From $S_{r_{\mathrm{opt}}}$ to $S_{30}$

UNSAM UNIVERSIDAD NACIONAL DE SAN MARTÍN
Karlsruhe Institute of Technology

- With rising zenith angle the distributions are shifted to lower signals due to the increasing attenuation of the air showers
- The horizontal line corresponds to a constant intensity which is clearly not achieved for the same value of $S_{r_{\mathrm{opt}}}$

$\downarrow$

applying the CIC correction

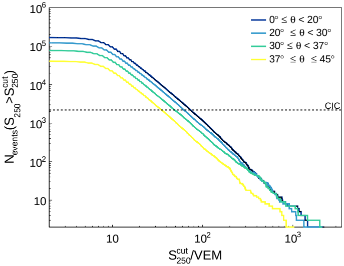


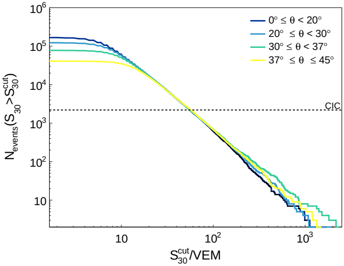

# From $S_{r_{\mathrm{opt}}}$ to $S_{30}$

UNSAM UNIVERSIDAD NACIONAL DE SAN MARTÍN

KIT Karlsruhe Institute of Technology

- With rising zenith angle the distributions are shifted to lower signals due to the increasing attenuation of the air showers
- The horizontal line corresponds to a constant intensity which is clearly not achieved for the same value of $S_{r_{\mathrm{opt}}}$

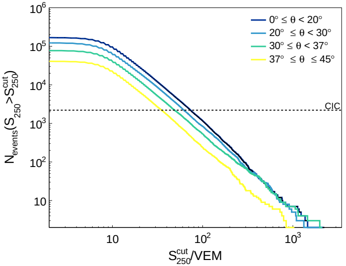


$\downarrow$

applying the CIC correction

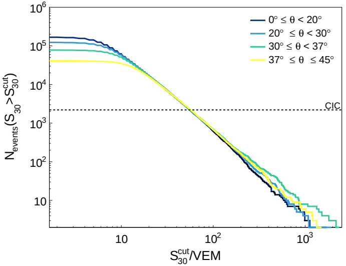


- The intensity corresponding to the chosen CIC is now attained at the same $S_{30}(E)$
- The systematic uncertainty of the energy estimate varies between 0% and 6% depending on zenith angle.

# From $S_{r_{\mathrm{opt}}}$ to $S_{30}$

- With rising zenith angle the distributions are shifted to lower signals due to the increasing attenuation of the air showers
- The horizontal line corresponds to a constant intensity which is clearly not achieved for the same value of $S_{r_{\mathrm{opt}}}$

$\downarrow$

applying the CIC correction

- The intensity corresponding to the chosen CIC is now attained at the same $S_{30}(E)$
- The systematic uncertainty of the energy estimate varies between 0% and 6% depending on zenith angle.

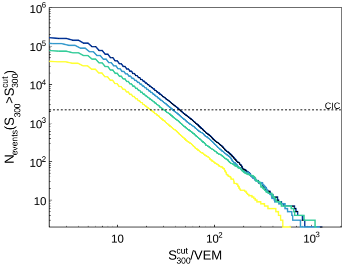


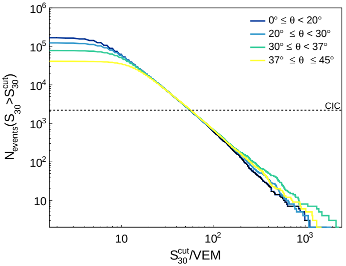

# Preliminary histogram

- used the recovered 6T5
- Old Offline reconstruction (S.Messina)
- clear break consistent with the second knee
- comms crisis period rejected (08/2018 - end 2019)

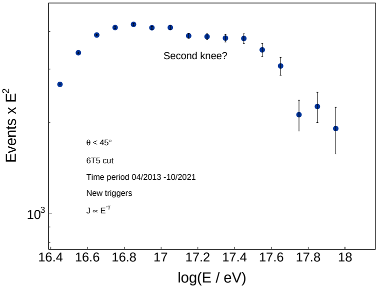

# Preliminary histogram

- used the recovered 6T5
- Old Offline reconstruction (S.Messina)
- clear break consistent with the second knee
- comms crisis period rejected (08/2018 - end 2019)

The fine-tuning of the SD-433 event reconstruction is still ongoing.

- weather-induced modulations on the measured signals
- calibration (SD-433 with SD-750)
- extend the spectrum to lower energies

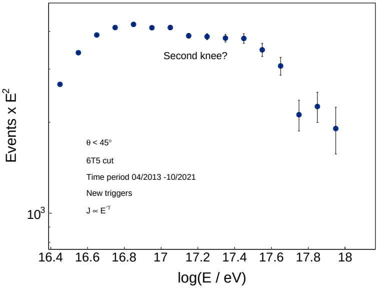

# Conclusions

UNSAM
UNIVERSIDAD NACIONAL DE SAN MARTÍN

Karlsruhe Institute of Technology

Summary:

- Silent stations fully restored
- SD433 Data set avaiable for the collaboration
- LDF slope $\beta$ parametrized as a function of $\sec\theta$ and $S_{250}$ (results presented at ICRC2021)
- SD-433 exposure $\Sigma \sim 4\ \mathrm{km}^2 \cdot \mathrm{yrs} \cdot \mathrm{sr}$
- Constant Intensity Cut correction

# Conclusions

Summary:

- Silent stations fully restored
- SD433 Data set avaiable for the collaboration
- LDF slope $\beta$ parametrized as a function of sec $\theta$ and $S_{250}$ (results presented at ICRC2021)
- SD-433 exposure $\Sigma \sim 4$ km$^2$ $\cdot$ yrs $\cdot$sr
- Constant Intensity Cut correction

Next step:

- SD-433 bad periods and comms crisis perdiod
- SD433 – SD750 energy calibration
- Second knee spectrum analysis

# Conclusions

Summary:

- Silent stations fully restored
- SD433 Data set avaiable for the collaboration
- LDF slope $\beta$ parametrized as a function of sec $\theta$ and $S_{250}$ (results presented at ICRC2021)
- SD-433 exposure $\Sigma \sim 4$ km$^2$ $\cdot$ yrs $\cdot$sr
- Constant Intensity Cut correction

Next step:

- SD-433 bad periods and comms crisis perdiod
- SD433 – SD750 energy calibration
- Second knee spectrum analysis

SD433 Group on-going analyses:

- SD433 – SD750 energy calibration (M. Roncoroni)
- bad periods, Angular and core resolutions (N.Gonzalez)
  NG et al, OCM2, Nov. 2020
- 433-750 trigger efficiency (G.Brichetto)

thank you!

# Exposure

The integrated SD-433 exposure as a function of time for the zenith angle range $0° \leq \theta \leq 45°$